Journal of Applied Sciences

ISSN 1812-5654

science alert

ANSInet
an open access publisher
http://ansinet.com

Journal of Applied Sciences 9 (8): 1544-1549, 2009
ISSN 1812-5654

Assessment of Artificially Induced Pressure Sores Using a Modified Fractal Analysis

[1]S. Moghimi, [1]M.H. Miran Baygi, [2]G. Torkaman and [1]A. Mahlooji Far
[1]Department of Biomedical Engineering,
[2]Department of Medical Science, Tarbiat Modares University, Tehran, Iran

Abstract: In this study, a guinea pig model has been developed for generation and monitoring of pressure sores. A system with pressure sensors and a suitable feedback was used for inducing pressure sores. High-frequency ultrasound images were taken from the wound site after tissue was released from the applied pressure for a 21 days period. Fractal properties of the selected windows were calculated, which leads to proposing a Modified Fractal Signature (MFS). The MFS proved to be an efficient measure for assessing the pressure sores. Exploiting the proposed idea, the progression of necrotic tissue could be studied. It is shown that this measure is also capable of evaluating the healing process of pressure sores.

Key words: Wound healing, high-frequency ultrasound imaging, guinea pig, modified fractal signature, covering blankets

INTRODUCTION

Reproducible assessment of wound healing has proven to be a complicated task. By studying the healing process, evaluation of drug effectiveness becomes possible, but this urges a certain need for more accurate assessment results (Rovee and Maibach, 2003). Efficient healing of wounds includes cells, matrices and complex chemicals, which act together in the healing process. The most popular assessment tool among clinicians consists of an acetate sheet to measure the wounds perimeter. For measurement of wound's volume, it is filled with a non-allergic liquid (Rovee and Maibach, 2003). These techniques along with other clinical methods, used for this specific purpose, are qualitative techniques which are irreproducible and suffer a lack of precision and most important of all are totally user-dependent.

The major part of the healing process occurs in deeper tissue layers, not visible to unequipped eyes. Therefore nondestructive monitoring of the phenomena seemed impossible until one or two decades ago. This fact is a more significant issue in dealing with pressure sores. These specific wounds occur when a constant pressure causes necrotic tissue to grow. Pressure sores have a major difference, comparing with acute wounds, that is unlike acute wounds they initiate in deeper skin layers and then progress to the superficial layers. Consequently, detection of early signs is still the main challenge. High-frequency ultrasound has been used for evaluation of wounds in general, since 1990. Forster *et al*. (1990) used high-frequency ultrasound (10-40 MHZ) backscattered signals to investigate surgery wounds. They concluded that the attenuation coefficient is also affected by factors other than the collagen fibers. Comparison of wound features, obtained from high-frequency ultrasound and histological images, verified the fact that the former technique is capable of demonstrating the dominant phenomena in the wound healing process. This was carried out by Rippon *et al*. (1998) in artificially induced acute wounds in guinea pigs. They also mentioned that the inflammation phase can be evaluated exploiting this approach, as this phase mostly consists of the bounding of collagen fibers (Rippon *et al*., 1999). Dyson *et al*. (2003) mentioned that the wound region may be more effectively extracted by high-frequency ultrasound than digital imaging.

In this study, artificially induced pressure sores have been studied using 22 MHZ B-mode ultrasound. Considering the fact that the qualitative assessment of these complicated wounds is inaccurate and subjective, the researchers have been trying to develop a quantitative measure based on modified fractal signature, which would show meaningful changes during the generation and healing processes of pressure sores. It is shown that modified fractal signature is a viable tool that can be employed for the assessment of the healing process of pressure sores.

Corresponding Author: Mohammad Hussain Miran Baygi, Department of Biomedical Engineering,, Tarbiat Modares University, P.O. Box 14115-111, Tehran, Iran
Tel: +98 (21) 82884331 Fax: +98 (21) 82884325

MATERIALS AND METHODS

Changes in picture properties as a result of changes in scale have been shown in previously published studies by Mandelbrot (1977, 1982) and Peleg *et al*. (1984). Fractal surface is an important feature in fractal objects, which in pictures may be calculated based on gray level values (Peleg *et al*., 1984). A perfect fractal object is self similar in all magnifications. In fact the slope of a fractal surface plotted versus the scale is known as fractal signature (Lekshmi *et al*., 2003). In this study a modified fractal signature is introduced based on the covering blanket technique. This technique is an extension of what Mandelbrot (1982) developed for measurement of coastlines. In the extension from curve to surface, all points in a distance ε from the gray level surface are considered, building a blanket of 2ε in diameter. The surface area is then calculated by dividing the blanket volume by 2ε. The covering blanket is defined by its upper and lower surfaces u_ε, b_ε. Assuming g (i, j) to be the gray level function, the initial upper and lower surfaces will be:

$$u_0(i, j) = b_0(i, j) = g(i, j) \quad (1)$$

Where: ε = 1, 2, 3.....

$$u_\varepsilon(i, j) = \max\begin{Bmatrix} u_{\varepsilon-1}(i, j) + 1, \max u_{\varepsilon-1}(m, n) \\ :|(m, n) - (i, j)| \le 1 \end{Bmatrix} \quad (2)$$

$$b_\varepsilon(i, j) = \min\begin{Bmatrix} b_{\varepsilon-1}(i, j) - 1, \min b_{\varepsilon-1}(m, n) \\ :|(m, n) - (i, j) \le 1| \end{Bmatrix} \quad (3)$$

where, m, n is the dimension of image points with distance less than one from point (i, j) which in fact build the immediate neighbors of (i, j). Eight-neighborhood may also be defined with the same expression. Blanket volume is computed as the difference between upper and lower surfaces (Peleg *et al*., 1984):

$$v_\varepsilon = \sum_{i,j} u_\varepsilon(i, j) - b_\varepsilon(i, j) \quad (4)$$

The fractal surface can then be calculated by one of the following definitions:

$$A(\varepsilon) = {}^{v_\varepsilon}\!/_{2\varepsilon} \quad (5)$$

$$A(\varepsilon) = {}^{[v_\varepsilon - v_{\varepsilon-1}]}\!/_{2} \quad (6)$$

Equation 6 provides a smoother value, while the definition in Eq. 5 adds up some noise, as it considers values from earlier scales. The surface provides a measure for oscillations of the covered texture. The window size can be appropriately selected based on the image size as well as the structure of the target texture. The surface shape converges to a smoother shape when the scale increases. Therefore, this technique is also referred to as a multi-resolution approach. The surface area increases when ε decreases and is approximated by the power law (Tang *et al*., 1997):

$$A(\varepsilon) = F\varepsilon^{2-D} \quad (7)$$

where, D stands for fractal dimension and F denotes a constant value. Taking the logarithm of both sides results in:

$$D = 2 - \frac{\log A(\varepsilon)}{\log(\varepsilon)} - \frac{\log F}{\log \varepsilon} \quad (8)$$

The fractal surfaces of two different scales may be used to omit the constant value F.

$$D = 2 - \frac{\log A(\varepsilon_1) - \log A(\varepsilon_2)}{\log \varepsilon_1 - \log \varepsilon_2} \quad (9)$$

When A(ε) is plotted versus ε on a log-log scale, the slope of the curve provides the fractal signature, S(ε). This value may be calculated by finding the best straight line connecting (log (ε-1), log (A(ε-1))), (log (ε), log (A(ε))) and (log (ε+1), log (A(ε+1))) and calculating its slope.

As mentioned earlier, one of the most important properties of fractal objects is their self-similarity in different magnifications. Therefore, the logarithmic curve should be a straight line for a fractal image. The difference in fractal signatures can be calculated using Eq. 10 (Shun *et al*., 1997).

$$D(i, j) = \sum_{\varepsilon} \left(S_i(\varepsilon) - S_j(\varepsilon)\right)^2 \log\left(\frac{\varepsilon + 1/2}{\varepsilon - 1/2}\right) \quad (10)$$

The echographic structure in high-frequency ultrasound images is noticeable by considering the changes in the gray level values in the Region of Interest (ROI). The MIN operator in Eq. 3 reduces the high gray level values and the rate of this action is highly related to the shape of these echoes. On the other hand the MAX operator reduces the background values, considering the distribution of echoes in the ROI as a dominant parameter. Exploiting this fact, the image may be considered to have two top and bottom views. In this case Eq. 4 is no longer appropriate for calculating the blanket volume. Instead it can be divided into two upper (v_ε^+) and lower (v_ε^-) volumes:

$$v_\varepsilon^+ = \sum_{i,j}\left(u_\varepsilon(i,j) - g(i,j)\right) \quad (11)$$

$$v_\varepsilon^- = \sum_{i,j}\left(g(i,j) - b_\varepsilon(i,j)\right) \quad (12)$$

It needs to be mentioned that the concept of upper and lower volumes was formerly introduced by Peleg *et al*. (1984). The surfaces are then introduced as follows:

$$A^+(\varepsilon) = v_\varepsilon^+ - v_{\varepsilon-1}^+ \quad (13)$$

$$A^-(\varepsilon-1) = v_\varepsilon^- - v_{\varepsilon-1}^- \quad (14)$$

Equation 10 may then be modified into Eq. 15 for calculating differences in fractal signatures (Peleg *et al*., 1984).

$$D(i,j) = \sum_\varepsilon \left\{\left[\left(S_i^+(\varepsilon) - S_j^+(\varepsilon)\right)^2 + \left(S_i^-(\varepsilon) - S_j^-(\varepsilon)\right)^2\right]\log\left(\frac{\varepsilon+1/2}{\varepsilon-1/2}\right)\right\} \quad (15)$$

It is noticeable that high frequency changes cause the blanket surface area to increase, which also augments the fractal signature. Considering the two upper and lower surfaces separately produces two fractal signature, S^- and S^+.

Here, the researchers claim that computing the lower blanket is not informative for this specific purpose. As the ROI consists of the echoes distributed in a dominant dark background, the lower surface will only experience a constant shift during the scale changes, resulting in a bias line. This is show in Fig. 1. Figure 1a represents a high-frequency ultrasound image taken for the purpose of this research. Figure 1b-e shows lower blanket surface in four different scales. After a few scales, the surfaces become so, alike that computing their difference would not be

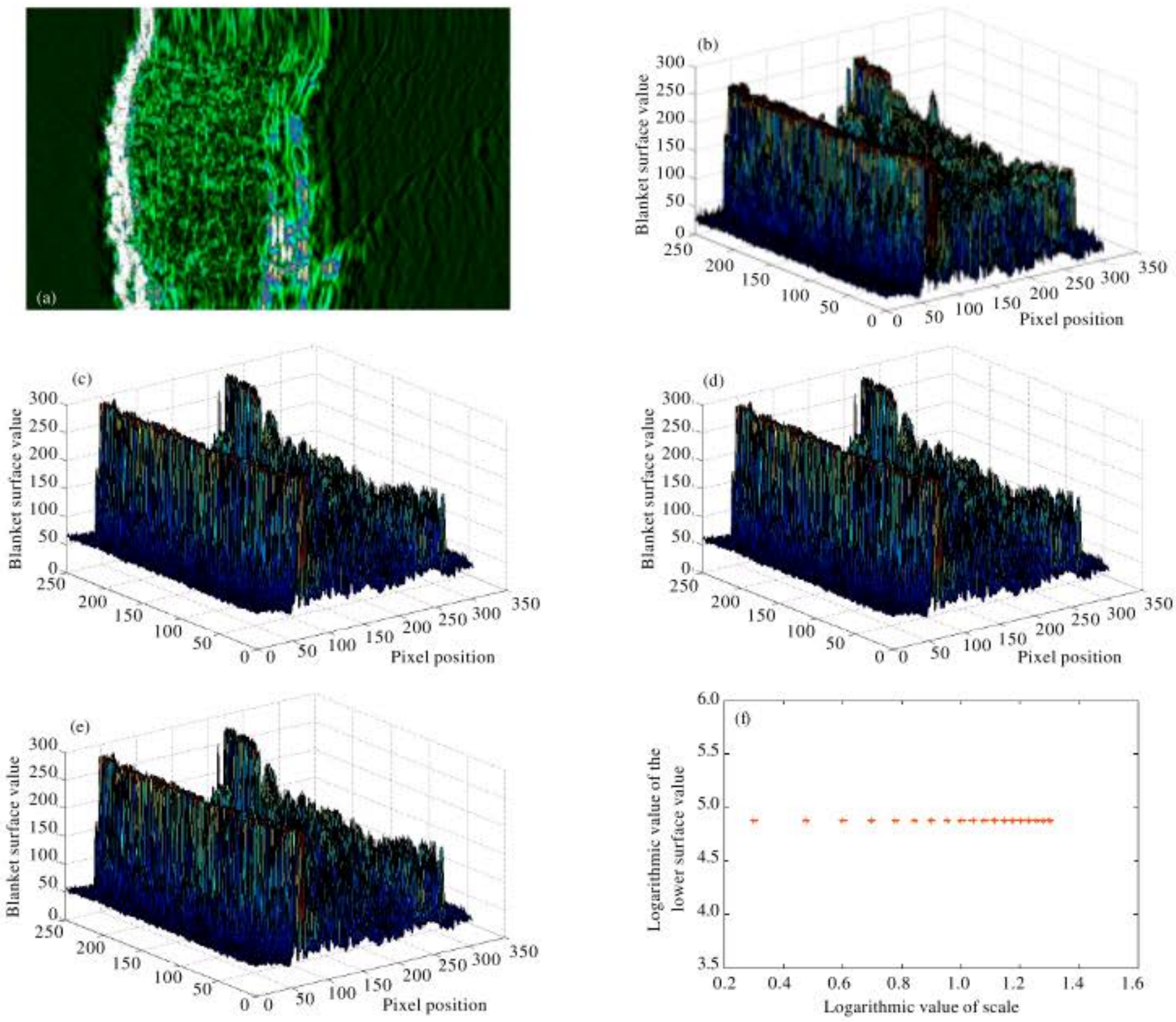

Fig. 1: (a) High-frequency ultrasound image, (b-e) Its lower covering blankets in four different scales and (f) The lower surface plotted versus scale in log-log scale

instructive at all. This fact is more emphasized in Fig. 1f, which is the plot of surface area versus scale in a log-log scale.

It was also mentioned earlier that the MAX operator (used in the calculation of the upper blanket) makes the distribution of echoes more important. In fact the distribution of echoes is what varies during the wound healing process. Considering the above explanations, the lower blanket may totally be neglected for the sake of operation time. From this point forward the fractal signature will change into the Modified Fractal Signature (MFS), which will be calculated from the slope of upper blanket surface plotted versus scale in a log-log scale.

Dunkin-Hartley guinea pigs were chosen for generation of pressure sores, based on the similarity of their skin tissue to that of human. All animals weighted between 300-450 g. The animals were anaesthetized during operation.

The developed system for generation of pressure sores included a feedback loop from the pressure sensor enabling us to control and monitor the applied pressure. Pressure was uniformly applied to a disk of diameter 0.75 cm. The animals were kept under pressure for 4-5 h. The ROI was then monitored for a 21 days period using a 22 MHZ B-mode ultrasound scanner (DUB_USB taberna pro medicum, Luneburg, Germany) in the controlled environment of the laboratory.

During the process of image acquisition the animals were kept in a restrainer to avoid the motion artifacts. The whole process was repeated 3 times to verify the image accuracy. The probe position was marked in the first image acquisition trial and then it was fixed in the same position during later sessions. Images were processed using MATLAB 7.3.

It needs to be mentioned that all the research steps are carried out in Tarbiat Modares University (Biomedical Engineering Department, 2008).

RESULTS AND DISCUSSIONS

The obtained images were considered as 3D functions for the sake of representation, as shown in Fig. 2.

Next the blanket surface was produced in a way that it covered the surface of the 3D functions. It needs to be mentioned that the size of the processing window was selected based on the disk diameter. Fig. 3a and b represent the surface of the upper blanket for the 1st and 20th scales, respectively. It is obvious that the surface converges to a smoother shape. Here onward, the surface would experience small changes in its shape, making the calculation of the blanket surface less helpful.

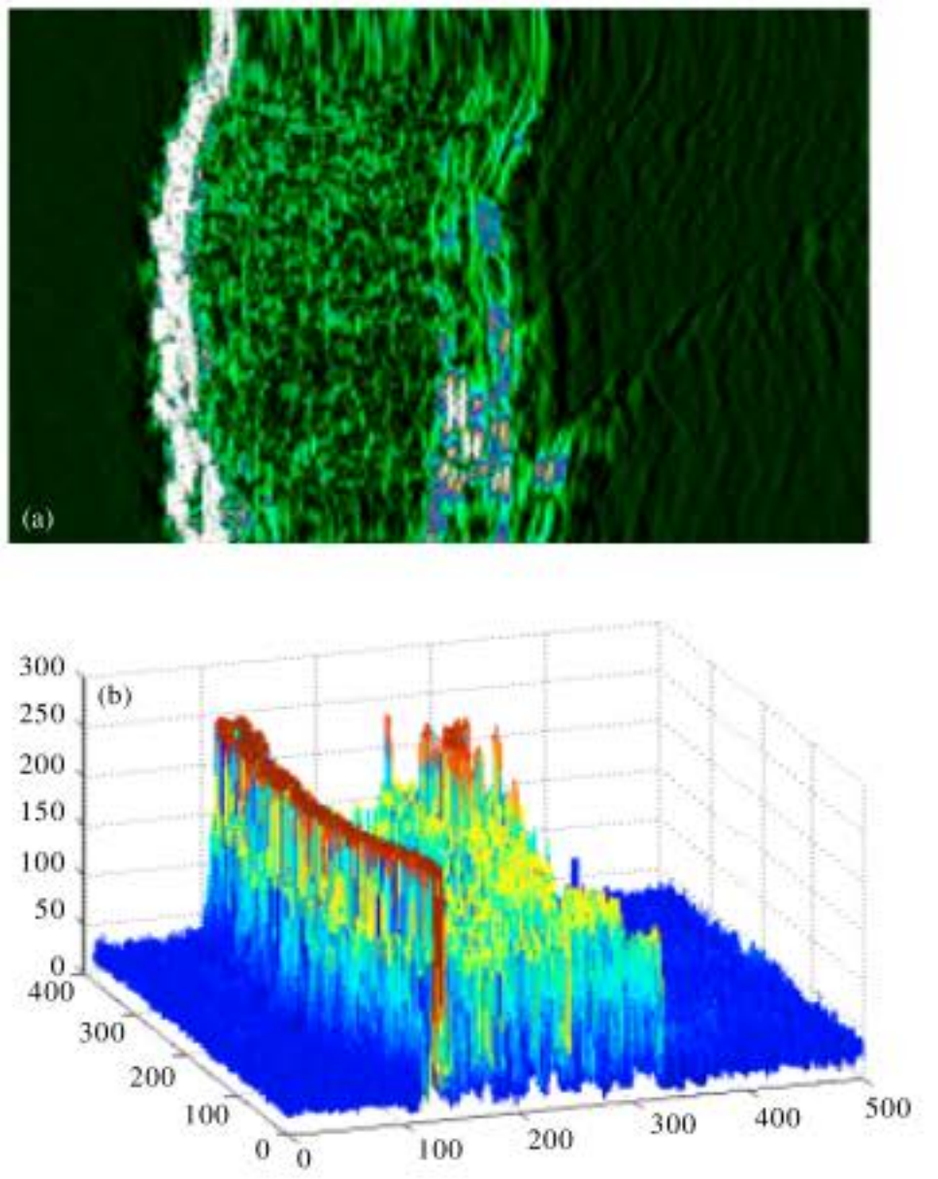

Fig. 2: (a) A High-frequency ultrasound image, (b) Its 3D graylevel function

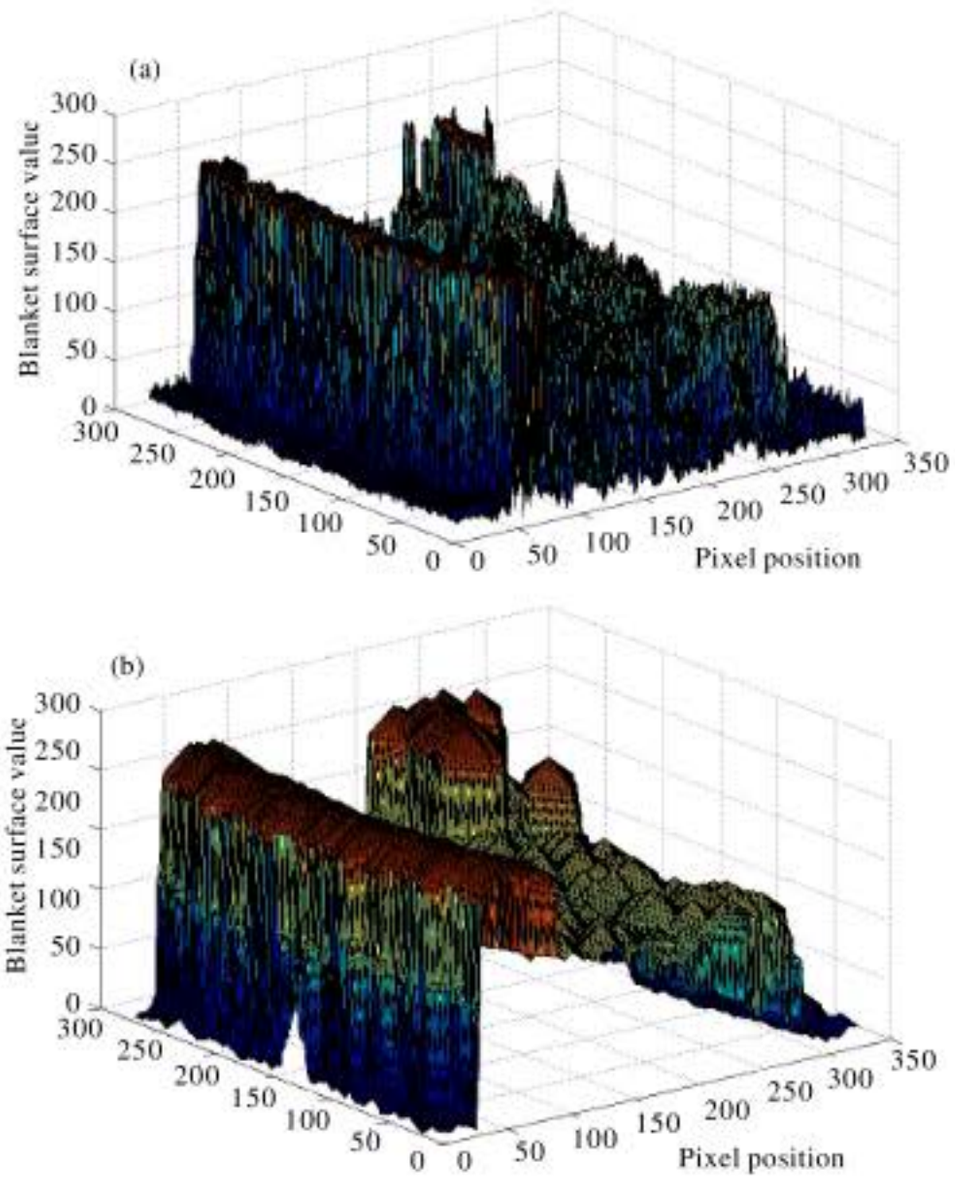

Fig. 3: The upper blanket surface (a) in the 1st and (b) in the 20th scales

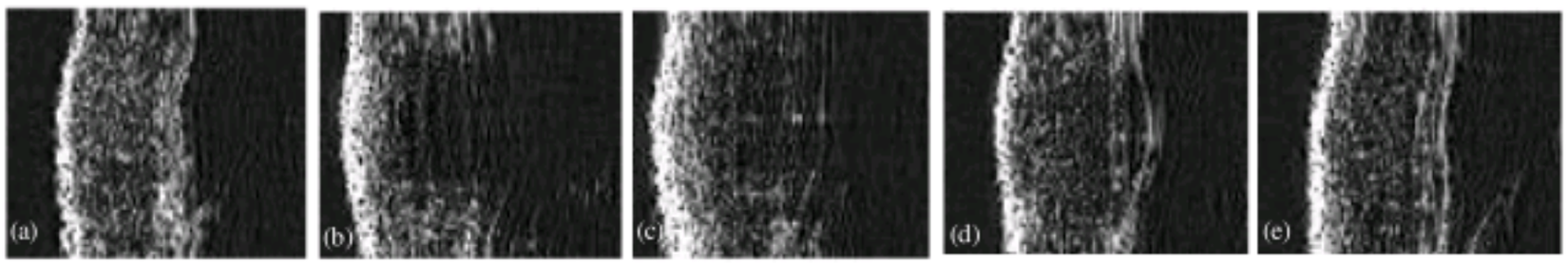

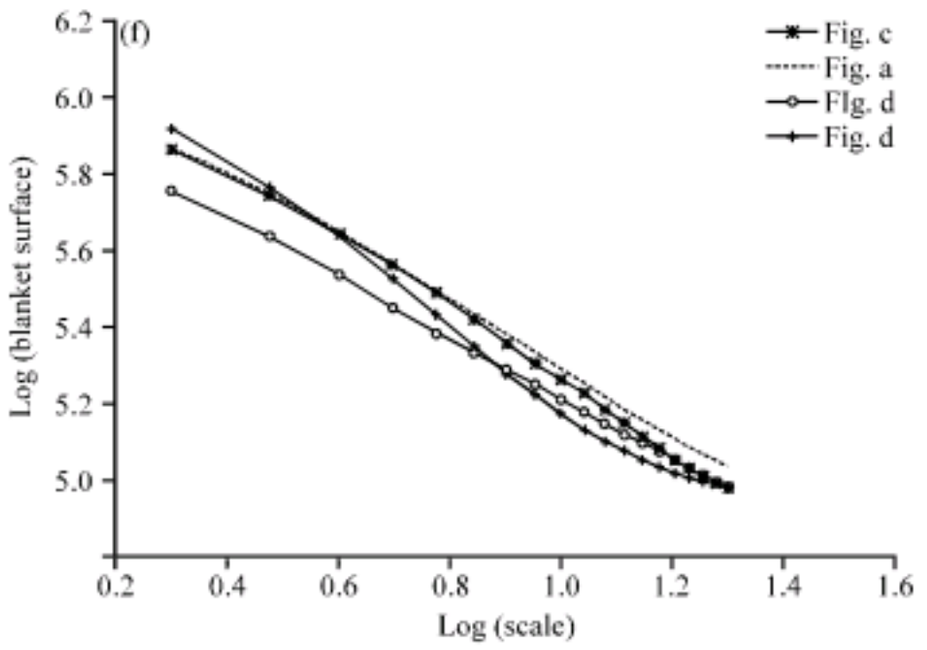

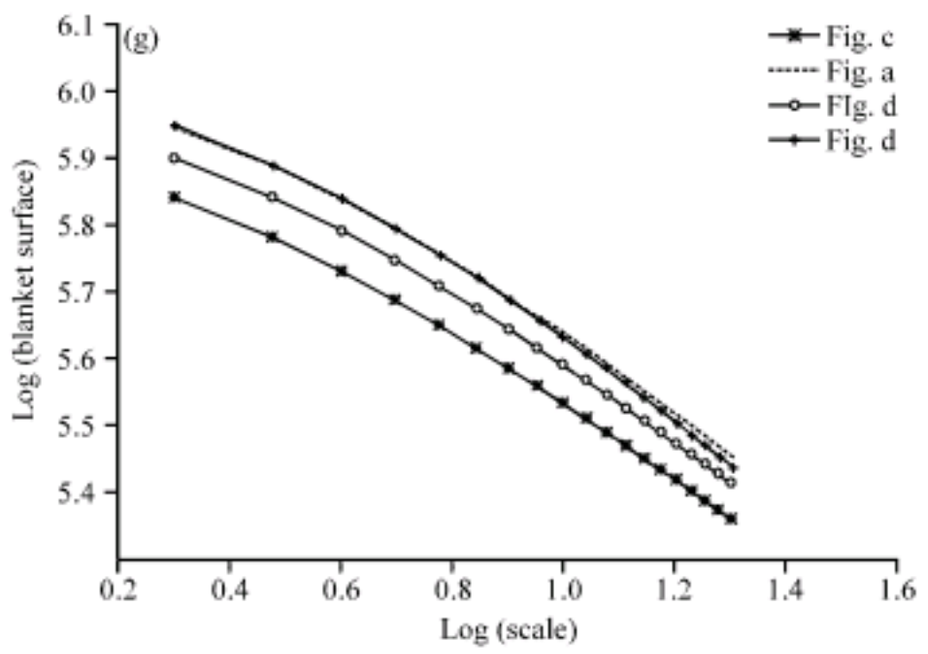

Fig. 4: (a-e) High-frequency ultrasound images of the process of wound generation and healing, (f) Blanket surface computed using Eq. 6 and plotted versus scale in a log-log scale, (g) Blanket surface computed using Eq. 5 and plotted versus scale in a log-log scale

The images of Fig. 4a-e show some of high-frequency ultrasound images, obtained during the generation and healing processes of pressure sores (they are sorted in a chorological order). The pixels other than those belonging to the ROI were neglected in order to reduce the processing time.

The blanket surface was calculated using the modified version of both Eq. 5 and 6 and plotted versus scale in a log-log scale for images of Fig. 4. In Fig. 4f the surfaces were` calculated using Eq. 6. Comparing this figure with Fig. 4g, it may be concluded that the differentiation form is more informative as in the latter figure no considerable slope changes can be recorded. This is due to the fact that blanket surfaces, calculated using Eq. 5, include the information of earlier surfaces as well. This causes small changes from one surface to the next one to disappear.

Figure 5 shows the difference in the MFS of healthy and damaged ROI for three different guinea pigs. Here, it needs to be explained that as the imaging procedure was initiated after the tissue was relieved from the applied pressure, it covered both generation and healing processes of pressure sores. The graphs in Fig. 5 have one thing in common; the MFS difference of the ROI from that of the healthy tissue increases as the pressure sore reaches its peak of severity by appearing in superficial layers. This difference decreases as the sores progress in the healing process. The interesting thing is that before

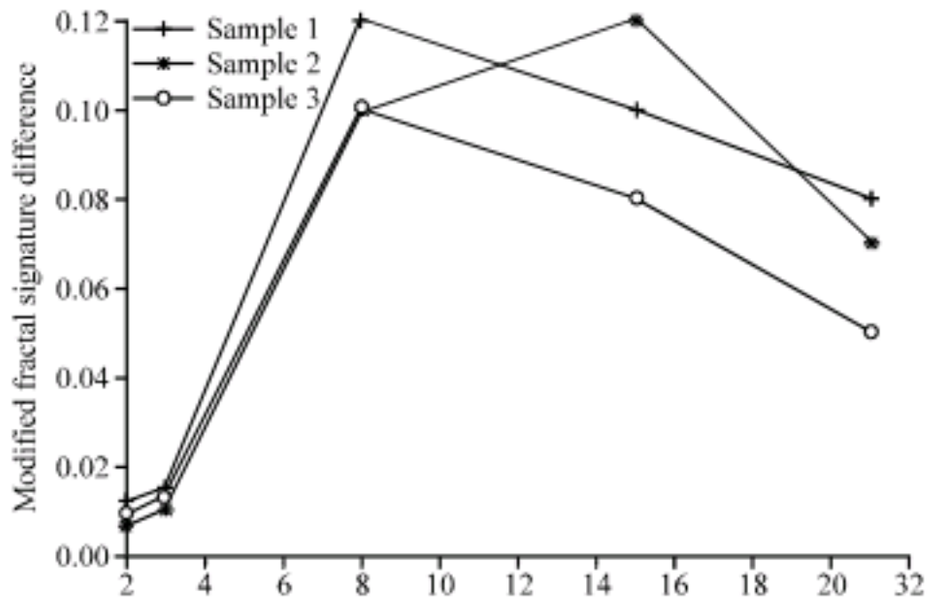

Fig. 5: Differences MFS of healthy and damaged tissue plotted versus days for 3 different guinea pigs

the pressure sores reach the superficial layers, they are, as mentioned earlier, invisible to the naked eyes, but the introduced parameter is able to assess the progression even in those early phases.

CONCLUSIONS

In this study an assessment tool was introduced for quantitative study of pressure sores. Fractal analysis was carried out which led to the MFS calculation. The determined measure was computed for the high-frequency

ultrasound images during the 21 days period. The results proved that the proposed assessment tool is able to monitor the progression of sores in tissue as well as the healing process. It was also shown that the measure is suitable for evaluation of sores even in early stages. Considering the fact that high-frequency ultrasound systems provide nondestructive monitoring of tissue, it may be concluded that the proposed approach is an appropriate quantitative tool for assessment of pressure sores. This approach may also be used for evaluating the effectiveness of the adopted treatment strategies, by measuring the extent to which the wound severity increase or decreases.

REFERENCES

Dyson, M., S. Moodley, L. Verjee, W. Verling, J. Weinman and P. Wilson, 2003. Wound healing assessment using 20 MHZ ultrasound and photography. Skin Res. Technol., 9: 116-121.

Forster, F.K., J.E. Oledrud, M.A. Henderson and A.W. Holmes, 1990. Ultrasonic assessment of skin and surgical wounds utilizing backscatter acoustic techniques to estimate attenuation. Ultrasound Med. Biol., 16: 43-53.

Lekshmi, S., K. Revathy and S.R. Prabhakaran-Nayar, 2003. Galaxy classification using fractal signature. Astronomy Astrophys., 405: 1163-1167.

Mandelbrot, B.B., 1977. Fractals: Form, Chance and Dimension. 1st Edn., WH Freeman and Co. San Francisco, ISBN: 0716704730.

Mandelbrot, B.B., 1982. The Fractal Geometry of Nature. 1st Edn., W.H. Freeman, San Francisco, CA., ISBN: 0716711869.

Peleg, S., J. Naor, R. Hartley and D. Avnir, 1984. Multiple resolution texture analysis and classification. IEEE Trans. Pattern Anal. Mach., Intell., 6: 518-522.

Rippon, M.G., K. Springett, R. Walmsley, K. Patrick and S. Millson, 1998. Ultrasound assessment of skin and wound tissue: Comparison with histology. Skin Res. Technol., 4: 147-154.

Rippon, M.G., K. Springett and R. Walmsley, 1999. Ultrasound evaluation of acute experimental and chronic clinical wounds. Skin Res. Technol., 5: 228-236.

Rovee, D.T. and H.I. Maibach, 2003. The Epidermis in Wound Healing, Chapter 7. 1st Edn., CRC Press Inc., USA., ISBN: 0849315611, pp: 125-140.

Shun, J., J. Li and T. Zhang, 1997. Detection of image fractal signature. Image Proc. Signal Proc. Synthetic Aperture Radar Remote Sensing, 3217: 342-351.

Tang, Y.Y., H. Ma, X. Mao, D. Liu and C.Y. Suen, 1997. A new approach to document analysis based on modified fractal signature. IEEE Trans. Knowledge Data Eng., 9: 7474-762.